Cortical recruitment of nonmuscle myosin II in early syncytial *Drosophila* embryos: its role in nuclear axial expansion and its regulation by Cdc2 activity

Anne Royou,[1] William Sullivan,[2] and Roger Karess[1]

[1]Centre National de la Recherche Scientifique, Centre de Génétique Moléculaire, 91198 Gif-sur-Yvette, France
[2]Department of Molecular, Cell, and Developmental Biology, Sinsheimer Labs, University of California, Santa Cruz, CA 95064

The nuclei of early syncytial *Drosophila* embryos migrate dramatically toward the poles. The cellular mechanisms driving this process, called axial expansion, are unclear, but myosin II activity is required. By following regulatory myosin light chain (RLC)–green fluorescent protein dynamics in living embryos, we observed cycles of myosin recruitment to the cortex synchronized with mitotic cycles. Cortical myosin is first seen in a patch at the anterocentral part of the embryo at cycle 4. With each succeeding cycle, the patch expands poleward, dispersing at the beginning of each mitosis and reassembling at the end of telophase. Each cycle of actin and myosin recruitment is accompanied by a cortical contraction. The cortical myosin cycle does not require microtubules but correlates inversely with Cdc2/cyclinB (mitosis-promoting factor) activity. A mutant RLC lacking inhibitory phosphorylation sites was fully functional with no effect on the cortical myosin cycle, indicating that Cdc2 must be modulating myosin activity by some other mechanism. An inhibitor of Rho kinase blocks the cortical myosin recruitment cycles and provokes a concomitant failure of axial expansion. These studies suggest a model in which cycles of myosin-mediated contraction and relaxation, tightly linked to Cdc2 and Rho kinase activity, are directly responsible for the axial expansion of the syncytial nuclei.

Introduction

Dynamic changes in the actin cytoskeleton drive cell shape changes and movements in all animal cells. Among the most prominent of these is cytokinesis, when the actin-myosin cytoskeleton undergoes rapid and dramatic reorganization to form the contractile ring. Precisely how this redistribution of actin and myosin filaments is spatially and temporally coordinated with the cell cycle is still unclear.

Regulating myosin motor activity is one way in which the actin cytoskeleton can be modified. Cytoplasmic myosin II (hereafter called myosin) is subject to both positive and negative regulation by phosphorylations at different sites on its regulatory myosin light chain (RLC)* (Sellers, 1991; Tan et al., 1992;

for review see Bresnick, 1999). Site-specific myosin phosphorylation (in vertebrate RLC at S19 and secondarily T18) by myosin light chain kinase (MLCK) or Rho kinase increases the actin-activated ATPase activity of myosin and also promotes the assembly of myosin into bipolar filaments. The importance of these phosphorylations for in vivo myosin function has been demonstrated in *Drosophila* (Jordan and Karess, 1997). In fibroblasts, S19 phosphorylation correlates with many cell shape changes, notably cytokinesis (Yamakita et al., 1994; DeBiasio et al., 1996; Matsumura et al., 1998).

Specific phosphorylations also inhibit myosin activity. In vitro phosphorylation at S1, S2, and S9 in vertebrate RLC inhibits the actin-activated ATPase activity of myosin by decreasing its binding affinity for actin and decreasing the affinity of RLC for MLCK. PKC and Cdc2 kinase (mitosis-promoting factor) phosphorylate these inhibitory sites in vitro, but the in vivo relevance of these phosphorylations is less clear. (Sellers, 1991; Satterwhite et al., 1992; Yamakita et al., 1994; Bresnick, 1999; Shuster and Burgess, 1999).

One model system for studying cell cycle–regulated cytoskeletal changes is the early *Drosophila* embryo. The first 13 divisions are rapid, synchronous, and occur without accompanying cytokinesis. The initial syncytial divisions oc-

---

The online version of this article contains supplemental material.

Address correspondence to Roger E. Karess, Centre de Génétique Moléculaire, Centre National de la Recherche Scientifique, Ave de la Terrasse, 91198 Gif sur Yvette, France. Tel.: 33-1-69-82-32-25. Fax: 33-1-69-82-31-50. E-mail: karess@cgm.cnrs-gif.fr

*Abbreviations used in this paper: A-P, anterior-posterior; Drok, *Drosophila* rho kinase; GFP, green fluorescent protein; GST, glutathione *S*-transferase; MHC, myosin heavy chain; MLCK, myosin light chain kinase; RLC, regulatory myosin light chain; TLCM, time-lapse confocal microscopy.
Key words: regulatory myosin light chain; nuclear axial expansion; Rho kinase; phosphorylation; cytokinesis

cur near the middle of the egg. During cycles 6 through 8, the cloud of dividing nuclei remains deep in the interior but expands along the long axis of the embryo. This results in a uniform distribution of nuclei along the anterior-posterior (A-P) axis at interphase of cycle 8. During cycles 8 and 9, the nuclei migrate toward the cortex. The first movement, termed nuclear axial expansion, requires a functional actin-myosin cytoskeleton (Zalokar and Erk, 1976; Hatanaka and Okada, 1991; von Dassow and Schubiger, 1994; Wheatley et al., 1995; Jordan and Karess, 1997), whereas the second movement, called cortical migration, is microtubule dependent and actin independent (Baker et al., 1993). The nuclei reach the cortex at the end of cycle 9. Once at the cortex, they undergo 4 additional rounds of synchronous divisions until during interphase of nuclear cycle 14 the plasma membrane invaginates around each nucleus to form the cellular blastoderm.

The process by which axial expansion occurs is unclear. One model proposes that the nuclei and their associated centrosomes rely on isotropic repulsion between aster microtubules to expand (Foe et al., 1993). This expansion is presumed to be confined to the long axis at the interior of the embryo by a dense network of cortical actin. A second model based on observation of actin distribution and cytoplasmic movement in fixed and living embryos argues that cycles of partial disassembly of the actin network around the nuclei generate cytoplasmic movements like that found in amoebic pseudopods (von Dassow and Schubiger, 1994). The resultant cytoplasmic streaming would then carry the nuclei along the A-P axis. Studies exploiting germline clones of mutations

in the *Drosophila spaghetti squash* (*sqh*) gene, which encodes the RLC, have demonstrated a requirement for myosin in nuclear axial expansion and suggest that regulation of myosin activity by activating phosphorylation of the RLC might be important (Wheatley et al., 1995; Jordan and Karess, 1997).

In this article, we employ time-lapse confocal microscopy (TLCM) of living embryos expressing fluorescent myosin to monitor myosin dynamics during these early embryonic events. We describe an extraordinary spatially and temporally regulated cycle of myosin recruitment to and dispersion from the cortex, beginning in early precortical divisions, first visible at the beginning of axial expansion, and continuing until the onset of cellularization. Each myosin recruitment is accompanied by a cortical contraction that appears to be responsible for the axial expansion of the nuclear cloud. We demonstrate that cortical myosin oscillation depends on Cdc2 activity but does not involve phosphorylation of the myosin RLC at the inhibitory phosphorylation sites. Rather, Cdc2 appears to act indirectly via Rho kinase to modulate phosphorylation of the RLC activating sites. We propose a model in which cycles of myosin-mediated cortical contraction and relaxation, regulated by Cdc2 activity, are responsible for the axial expansion of the syncytial nuclei.

Results

Myosin undergoes cycles of cortical recruitment and dispersal in concert with mitotic cycles

To better understand the role that myosin plays in promoting nuclear axial expansion, we followed myosin dynamics in vivo
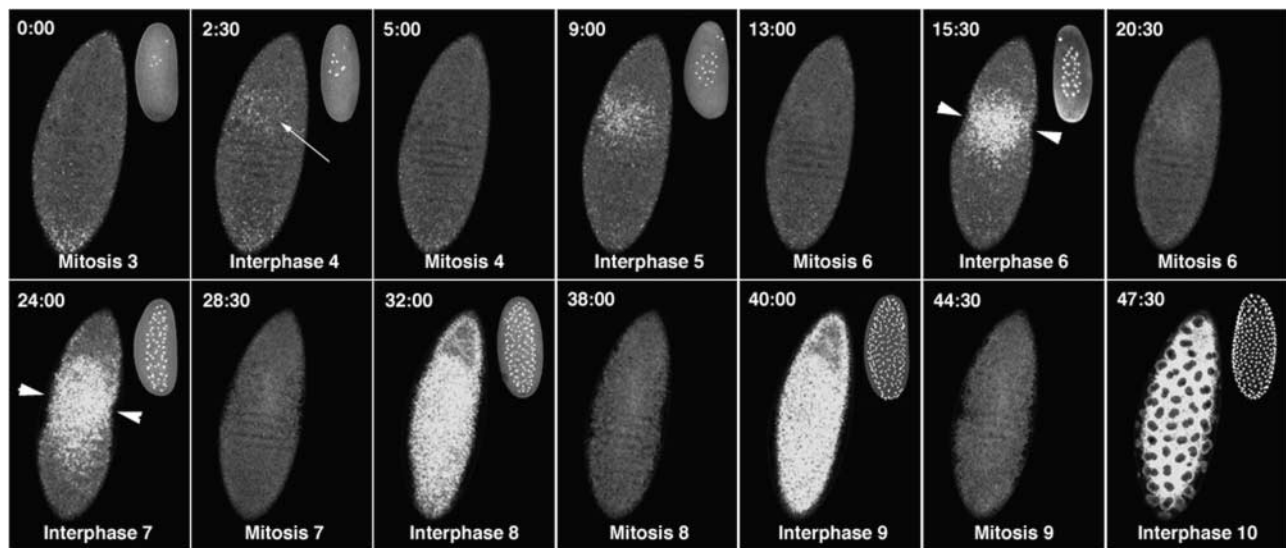

Figure 1. **Myosin dynamics in vivo during precortical divisions: cortical myosin distribution coincides with nuclear position.** The surface of an early RLC–GFP embryo was examined by TLCM. The anterior pole is at the top. Video 1 (available at http://www.jcb.org/cgi/content/full/jcb.200203148/DC1) begins at mitosis of cycle 3 (based on the time of embryo development) and ends at cycle 10 (the last panel) when nuclei reach the cortex and myosin reorganizes around them. No fluorescence signal is detectable at the cortex before cycle 4. At interphase of cycle 4, a faint patch of cortical fluorescence appears just anterior to the center (2:30, arrow). The fluorescent patch undergoes cycles of appearance and disappearance roughly every 7 or 8 min, which corresponds to the length of the precortical nuclear cycle. With each succeeding cycle, the patch of cortical fluorescence intensifies and spreads in both directions until interphase of cycle 8, when it covers the entire embryo (the apparent absence of myosin from the extreme anterior end of this embryo in interphases 8 and 9 is caused by a surface deformation pushing this region out of the focal plane). At interphase 10, the nuclei (black holes) arrive at the cortex, and the myosin fluorescence reorganizes around them. The insets present fixed embryos stained with antihistone antibody to visualize the position of the nuclear cloud at each cycle for comparison with the distribution of the RLC–GFP fluorescence. Each inset is a projection of confocal stacks of a single embryo in order to visualize all the nuclei.
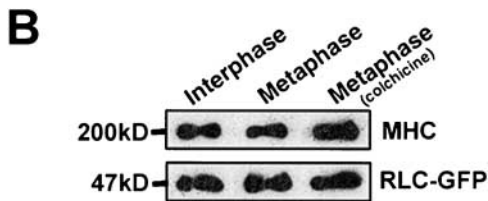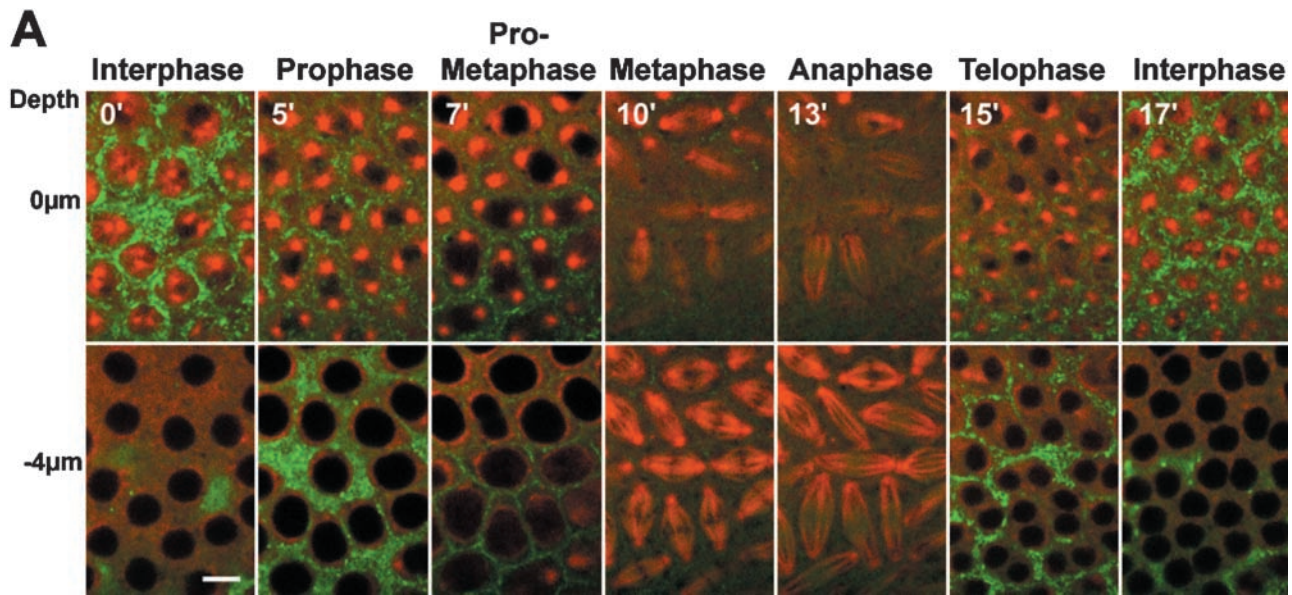
Figure 2. **Cycles of myosin recruitment to the cortex correlate with the mitotic cycle and are not caused by proteolytic degradation.** (A) All panels are from scanning confocal videos (videos 2 and 3 available at http://www.jcb.org/cgi/content/full/jcb.200203148/DC1) of RLC–GFP (green) embryos injected with rhodamine-tubulin (red). Two focal planes are shown. The left column is an apical surface view, and the right is the corresponding basal view, 4 μm below the surface. The embryo was followed from interphase of cycle 13 through interphase of cycle 14. The RLC–GFP fluorescence (green) strongly stains the cortex at interphase and is organized into broad rings surrounding each pair of centrosomes (red). During prophase, the fluorescence is found primarily at the basal plane corresponding to the tip of the invaginating metaphase furrow. The fluorescence dramatically decreases at prometaphase after nuclear envelope breakdown. A diffuse myosin signal remains associated with the spindle throughout metaphase and anaphase. The RLC–GFP fluorescence begins to reappear first at the basal level around each mitotic figure during telophase. Finally, the RLC–GFP returns once again to the apical plane after furrow regression, surrounding each new pair of centrosomes. Bar, 4 μm. (B) A Western blot of embryo extracts prepared from syncytial RLC–GFP embryos at interphase (first lane), at metaphase (second lane), and embryos blocked in metaphase for 15 min with colchicine (third lane), and probed with anti-MHC and anti-GFP. No quantitative difference in the amount of either MHC and RLC–GFP was detectable.

in the early embryo as revealed by a fully functional RLC–green fluorescent protein (GFP) fusion protein and TLCM. Fig. 1 (and video 1 available at http://www.jcb.org/cgi/content/full/jcb.200203148/DC1) presents a single optical section of a surface view of an RLC–GFP embryo during mitotic cycles 3–10. We found that cortical myosin is highly dynamic and undergoes cycles of recruitment every 7–8 min, which coincides with the length of the precortical nuclear cycle. Myosin first appeared at the cortex at cycle 4 in a faint patch centered at ∼1/3 egg length from the anterior (Fig. 1, 2:30, arrow). With each subsequent division cycle, the patch enlarged, spreading poleward until by cycle 8 the patch covered the entire cortex. A cortical contraction accompanied each cycle of myosin accumulation (particularly evident in interphase 6 and interphase 7 [Fig. 1, arrowheads]). No such cortical contractions occur in sqh[1] mutant germline clones (unpublished data). The insets in each panel of Fig. 1 present fixed embryos with nuclei stained with antihistone antibodies at similar cycles of mitosis and show that the cortical patches of myosin coincide roughly to the position of the syncytial nuclear cloud as it extends along the A-P axis.

Studies of fixed embryos by Foe et al. (2000) have shown that once the nuclei reach the cortex at interphase of cycle 10 myosin reorganizes around the nuclei and is completely excluded from the actin-rich caps above the nuclei. Foe et al.

(2000) also reported that at each of the four blastoderm metaphases, while actin concentrated in the metaphase furrow, myosin disappeared from the cortex. To obtain a real-time description of myosin dynamics with respect to the cell cycle, we monitored RLC–GFP myosin behavior in living embryos during the later syncytial divisions 10–13. RLC–GFP embryos were injected with rhodamine-tubulin to follow simultaneously myosin and microtubule dynamics. Fig. 2 A (and videos 2 and 3 available at http://www.jcb.org/cgi/content/full/jcb.200203148/DC1) presents two optical sections: an apical plane and a basal plane 4 μm deeper, in order to follow myosin organization during metaphase furrow invagination. Interphase myosin is found in the apical plane surrounding each nucleus in broad rings and is excluded from the actin caps (Fig. 2 A and Fig. 1, Interphase 10). During prophase, myosin is reduced apically but is abundant 4 μm below at the basal plane (Fig. 2 A, 5 min). These live studies agree with fixed studies of Foe et al. (2000), indicating that myosin is concentrated at the leading edge of the invaginating furrow. However, after nuclear envelope breakdown at prometaphase myosin rapidly declines throughout the cortex. By metaphase, although robust actin-based furrows surround each spindle, the levels of cortical myosin are greatly reduced. Only during late anaphase and telophase when the furrows are rapidly re-

ceding does cortical myosin reappear, beginning basally. By Western blot, no differences in quantity of either myosin heavy chain (MHC) or RLC–GFP were detected in extracts of embryos at interphase, metaphase, or in metaphase-arrested embryos after treatment with colchicine (Fig. 2 B), suggesting that cyclic disappearance of cortical myosin during mitosis is not due to cycles of proteolytic degradation. Thus, the strongly reduced signal of GFP at the cortex during mitosis is most likely due to a disassembly of myosin molecules from the cortex and their dispersion into the cytoplasm.

The cycles of myosin recruitment to the cortex do not require microtubules

There is evidence that the redistribution adopted by cortical myosin around the nuclei when they reached the cortex at cycle 10 is influenced by the disposition of microtubules (Foe et al., 2000). However, it is unclear whether microtubules are directly involved in the cortical recruitment of myosin during telophase. We examined this question by injecting 1 mM colchicine into anaphase RLC–GFP embryos precisely during early anaphase. 2 min after colchicine injection, the mitotic spindle had completely disappeared (Fig. 3 A; video 4 available at http://www.jcb.org/cgi/content/full/jcb.200203148/

DC1). However, the embryos continued to exit mitosis, and 4 min after injection, as the nuclear envelope reformed at telophase, myosin once again accumulated at the cortex. Injection of colchicine during interphase of cycle 12 caused embryos to arrest at the subsequent metaphase. In such embryos, myosin dispersed normally at entry into mitosis and remained dispersed during the metaphase arrest (Fig. 4 A, 10′ colchicine). These results argue that myosin recruitment to and dispersion from the cortex do not require microtubules.

Cycles of myosin recruitment to the cortex are directly linked to cycles of Cdc2 activation and inactivation

The above studies demonstrate that myosin recruitment is linked to the mitotic cycle and therefore might be directly influenced by Cdc2 activity. To test this correlation, we perturbed Cdc2 activity in a number of ways and monitored the effects on myosin behavior.

Glutathione *S*-transferase–cyclin B. To test whether the degradation of cyclin B at anaphase is required for cortical myosin recruitment, we made use of a recombinant *Drosophila* cyclin B protein fused by its NH_2 terminus to glutathione *S*-transferase (GST). This GST–cyclin B fusion protein has been shown to be stable in vivo (Su et al., 1998).
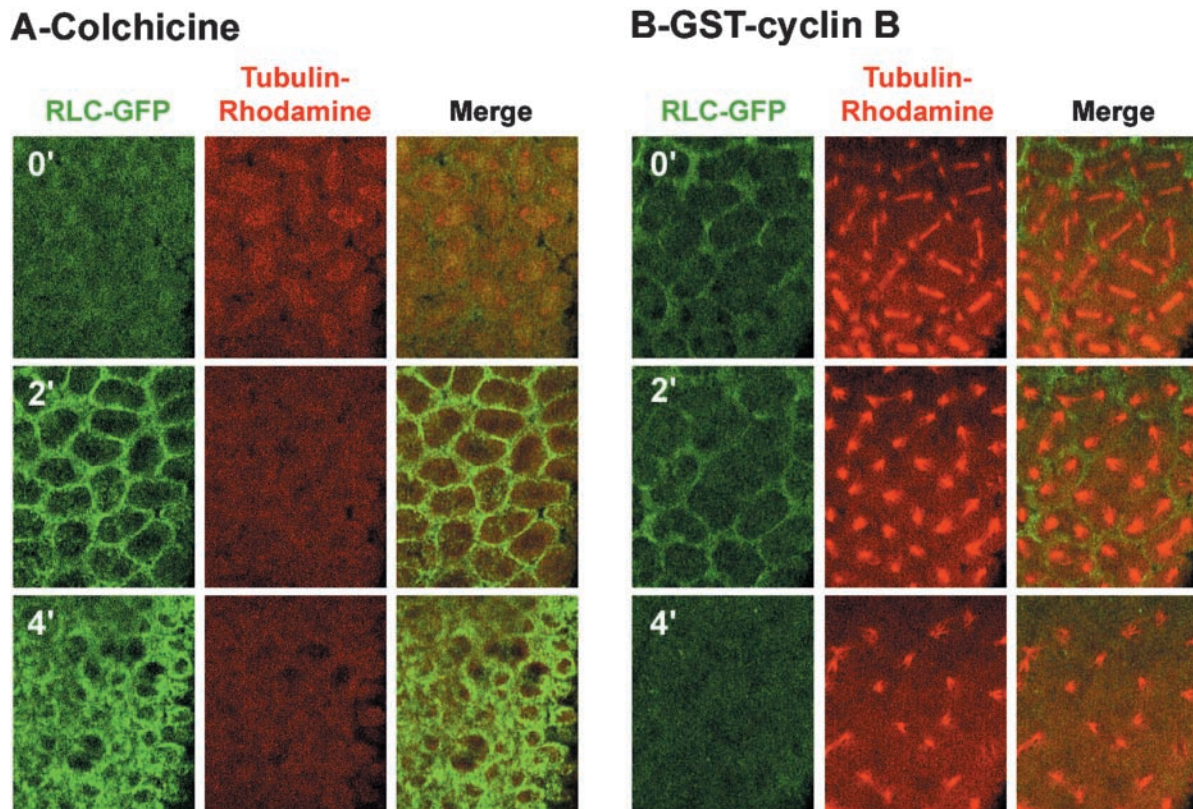

Figure 3.   **The cycle of myosin recruitment to the cortex does not depend on microtubules but does depend on cyclin B degradation.** All panels are from scanning confocal videos (videos 4 and 5 available at http://www.jcb.org/cgi/content/full/jcb.200203148/DC1) of RLC–GFP embryos injected with rhodamine-tubulin. In each case, the products were injected precisely during the anaphase stage of a syncytial cycle. (A) Colchicine injection (1 mM) does not prevent myosin recruitment to the cortex. The effect of colchicine on the mitotic spindle (red) can be seen: the spindle disappears almost immediately after drug treatment. Despite this, recruitment of myosin (green) to the cortex during telophase and interphase is unaffected. See video 4 available at http://www.jcb.org/cgi/content/full/jcb.200203148/DC1. (B) GST–cyclin B fusion protein inhibits myosin recruitment at the cortex at telophase. The first frame (0 min) was recorded a few seconds after GST–cyclin B injection. At this time, myosin begins to accumulate at telophase, but instead of remaining the cortical recruitment is reversed, and myosin is completely dispersed again 4 min after injection. See video 5 available at http://www.jcb.org/cgi/content/full/jcb.200203148/DC1.
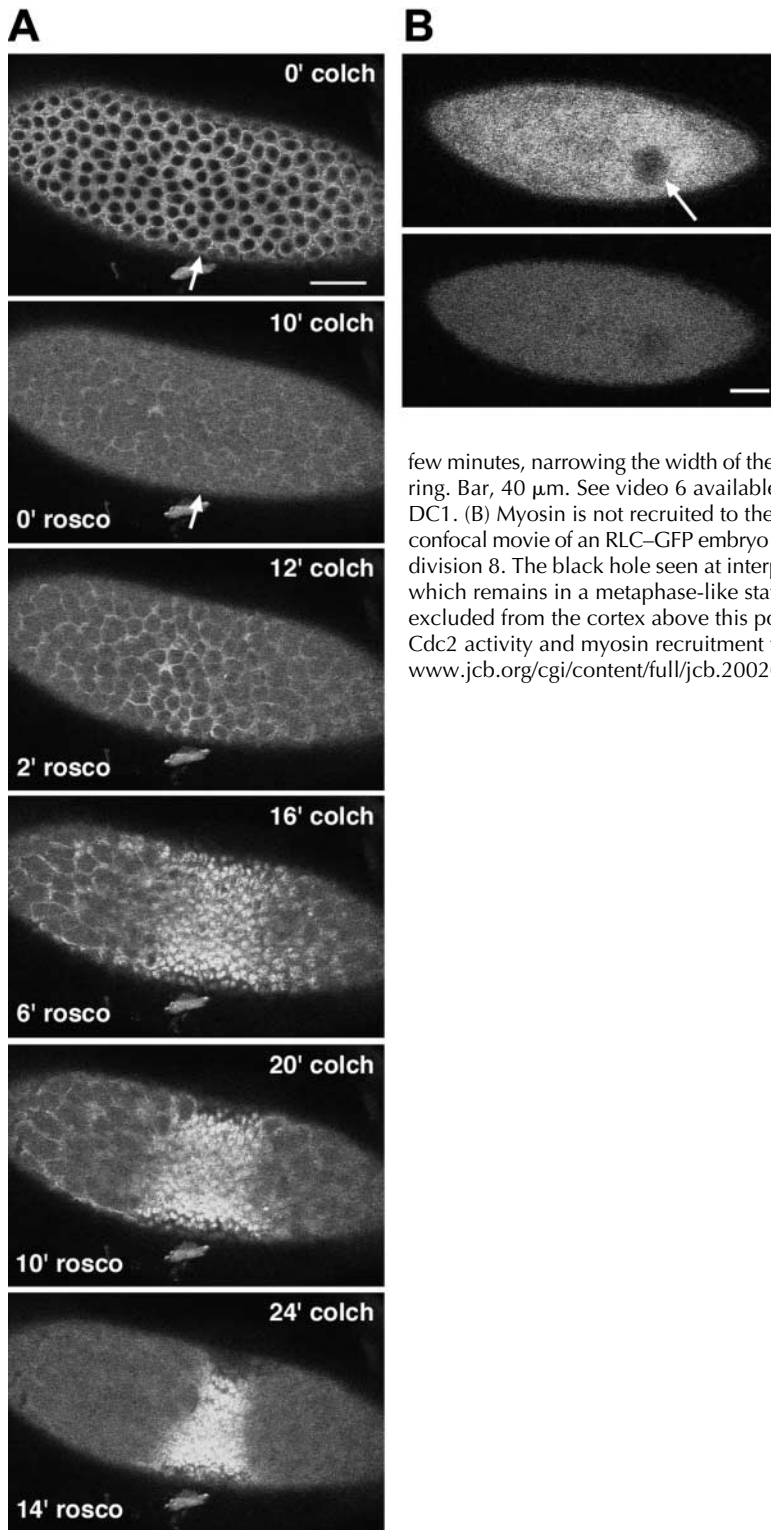
A

0' colch

10' colch

0' rosco

12' colch

2' rosco

16' colch

6' rosco

20' colch

10' rosco

24' colch

14' rosco

B

Figure 4. **Cortical myosin recruitment is inhibited by Cdc2 activity.** (A) Cdc2 inactivation by roscovitine leads to cortical myosin recruitment. An interphase 12 RLC–GFP embryo with the typical rings of cortical myosin surrounding each nucleus was injected with colchicine (1 mM, first frame, arrow) and monitored by TLCM. 10 min after colchicine injection, the whole embryo had arrested at metaphase with the cortical myosin diffused into the cytoplasm. At this time, roscovitine (10 mM) was injected into the same wound (arrow). 2 min later, myosin began to reaccumulate at the cortex at the site of roscovitine injection. The cortex increased in fluorescence dramatically over the next 6 min. 10 min after roscovitine injection, the cortex began to contract exactly within the newly recruited myosin patch. The contraction of cortical myosin continued over the next few minutes, narrowing the width of the patch and producing a structure reminiscent of a contractile ring. Bar, 40 μm. See video 6 available at http://www.jcb.org/cgi/content/full/jcb.200203148/DC1. (B) Myosin is not recruited to the cortex above the polar body. Two frames of a scanning confocal movie of an RLC–GFP embryo at interphase (top) and metaphase (bottom) during precortical division 8. The black hole seen at interphase (arrow) corresponds to the position of the polar body, which remains in a metaphase-like state even though the rest of the embryo is cycling. Myosin is excluded from the cortex above this polar body, again revealing the inverse correlation between Cdc2 activity and myosin recruitment to the cortex. Bar, 40 μm. See video 7 available at http://www.jcb.org/cgi/content/full/jcb.200203148/DC1.

We injected this stabilized form of cyclin B into syncytial RLC–GFP embryos at late anaphase just before cortical myosin recruitment (Fig. 3 B; video 5 available at http://www.jcb.org/cgi/content/full/jcb.200203148/DC1). At this point in the mitotic cycle, Cdc2 is normally inactivated by the APC-dependent degradation of endogenous cyclin B (Su et al., 1998). Fig. 3 B (top, 0′) corresponds to early telophase, just a few seconds after GST–cyclin B injection. Myosin has begun to reaccumulate normally around each mitotic figure, and nuclear envelopes have reformed. However, 2 min after injection nuclei reentered mitosis, and by 4 min (Fig. 3 B; bottom) myosin had completely disappeared from the cortex. Thus, ectopic activation of Cdc2 leads rapidly to the dispersal of cortical myosin.

Roscovitine injection. Roscovitine is an inhibitor of cyclin-dependent kinases Cdc2, Cdk2, and Cdk5 (Meijer et al., 1997). That this drug was capable of inhibiting cdks in syncytial fly embryos was shown in preliminary experiments where

injection of roscovitine during interphase of cycle 13 delayed the next mitotic entry at the site of injection by 10–12 min (unpublished data). By microinjecting roscovitine into colchicine-treated, metaphase-arrested embryos (with elevated Cdc2 activity), we therefore expected to inactivate the Cdc2 at the site of injection. For this experiment, RLC–GFP embryos were filmed before, during, and after the drug treatments (Fig. 4 A; video 6 available at http://www.jcb.org/cgi/content/full/jcb.200203148/DC1). Embryos were first injected during interphase of cycle 12 with 1 mM colchicine, which rapidly diffused through the embryo, causing a uniform and prolonged arrest in metaphase (Fig. 4 A, first and second frames). 10 min after colchicine injection, 10 mM roscovitine was injected in the same hole (Fig. 4 A, second frame, arrow). 2 min after roscovitine injection (Fig. 4 A, third frame), myosin began to accumulate at the cortex near the site of injection, increased rapidly for the next 6–8 min, and was accompanied by a strong cortical contraction in the myosin patch (Fig. 4 A, fifth and sixth frames). We conclude that inhibition of Cdc2 by roscovitine leads to the recruitment of myosin at the cortex.

Exclusion of cortical myosin near the polar body. During the precortical mitotic cycles of RLC–GFP embryos, a black hole can be seen in which cortical myosin is excluded even during interphase (Fig. 4 B; video 7 available at http://www.jcb.org/cgi/content/full/jcb.200203148/DC1). This black hole corresponds to the position of the polar body, the products of female meiosis, which do not contribute to the gamete. After meiosis, the polar body migrates near the cortex, arrested in a metaphase-like state with condensed chromosomes and elevated Cdc2 kinase activity (Su et al., 1998) but without a proper mitotic spindle (Foe et al., 1993). The exclusion of myosin from the cortex just above the polar bodies supports a role for Cdc2 in regulating the recruitment of cortical myosin and also suggests that the inhibitory range of Cdc2 activity on myosin recruitment is ∼30 μm. (Exclusion of myosin from the polar body was also described by Foe et al. [2000] but interpreted differently [see Discussion].)

The RLC is not a target of Cdc2 inhibitory phosphorylation

Phosphorylation of serines 1 and 2 and threonine 9 in vertebrate smooth and nonmuscle RLC inhibits the actin-activated ATPase activity of myosin by decreasing its affinity for F-actin and also decreases the affinity of the RLC for MLCK (Bengur et al., 1987; Ikebe and Reardon, 1990). Purified Cdc2 reportedly phosphorylates these inhibitory sites of the vertebrate RLC in vitro (Satterwhite et al., 1992), and in living cells their phosphorylation correlates with times of activated Cdc2 (Yamakita et al., 1994).

To test the importance of these residues for myosin function in *Drosophila*, we made a transgene expressing an RLC in which all the demonstrated (S1, S2, and T11) and putative sites (T5 and T12) involved in inhibiting myosin activity were replaced by alanines (Fig. 5 A). This transgene, called *sqh-5XA*, nevertheless fully rescued the null *sqh^AX3* mutation when present in a single copy in the genome. Therefore, phosphorylation of these sites is not essential for myosin function in vivo in *Drosophila*.

The cortical myosin cycle in early embryos expressing only this mutant RLC appeared to be identical to that seen in the
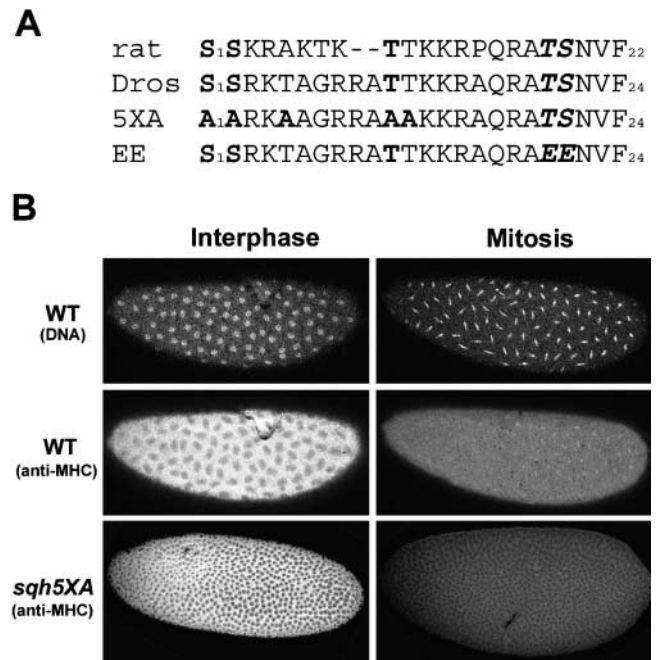

A

```
rat    S₁SKRAKTK--TTKKRPQRATSNVF₂₂
Dros   S₁SRKTAGRRATTKKRAQRATSNVF₂₄
5XA    A₁ARKAAGRRAAAKKRAQRATSNVF₂₄
EE     S₁SRKTAGRRATTKKRAQRAEENVF₂₄
```

B

Figure 5. **Cycles of myosin cortical recruitment are not caused by inhibitory phosphorylation of the RLC.** (A) The NH₂ terminal sequence of RLC of rat aortic smooth muscle myosin (Taubman et al., 1987), *Drosophila* nonmuscle myosin (Karess et al., 1991), the mutant *sqh-5XA,* and mutant *sqh-EE*. The inhibitory sites demonstrated to be phosphorylated in vitro by PKC or Cdc2 are in bold. In the construct *sqh-5XA*, all five potentially phosphorylatable serines and threonines have been mutated to alanines (bold). The *sqh-5XA* transgene can fully complement a *sqh*-null mutation, producing viable fertile flies expressing only mutant RLC. The *sqh-E20E21* transgene has replaced the two activating phosphorylation sites (italic) with phosphomimetic glutamate residues. This transgene can rescue the nuclear axial expansion defect of sqh¹ and sqh^AX3 germline clones (unpublished data). (B) At interphase, both WT and Sqh5XA embryos show strong immunostaining of cortical myosin (left), whereas during mitosis this staining strongly decreases (right). Wild-type and sqh5XA embryos were fixed and stained with anti-MHC (middle and bottom, respectively) and propidium iodide (top; only the wild-type is shown), and sorted according to their mitotic stage. The anti-MHC antibody signal is identical to that seen for RLC–GFP fluorescence in the wild type, confirming that RLC–GFP is a good marker for myosin in vivo. No difference is found between wild-type and sqh5XA embryos, demonstrating that myosin lacking the RLC inhibitory phosphorylation sites still undergoes cycles of recruitment at interphase and dispersion at mitosis.

wild-type embryo or RLC–GFP embryos (Fig. 5 B) with a strong anti-MHC staining at the cortex during interphase and a weak signal during metaphase. We conclude that phosphorylation at these sites by Cdc2, or any other kinase, cannot explain the cyclic recruitment and dispersion of cortical myosin.

The RLC activating sites regulated by Rho kinase are involved in cortical recruitment and dispersion

Phosphorylation of the RLC activating sites (S19 and secondary T18 for vertebrates and S21 and T20, respectively, for *Drosophila*) is required for myosin motor activity and promotes the assembly of myosin into bipolar filaments (for review see Tan et al., 1992). The phosphorylation at these sites also correlates with active cell shape changes (Sellers, 1991; Amano et al., 1996; DeBiasio et al., 1996; Jordan and Karess,
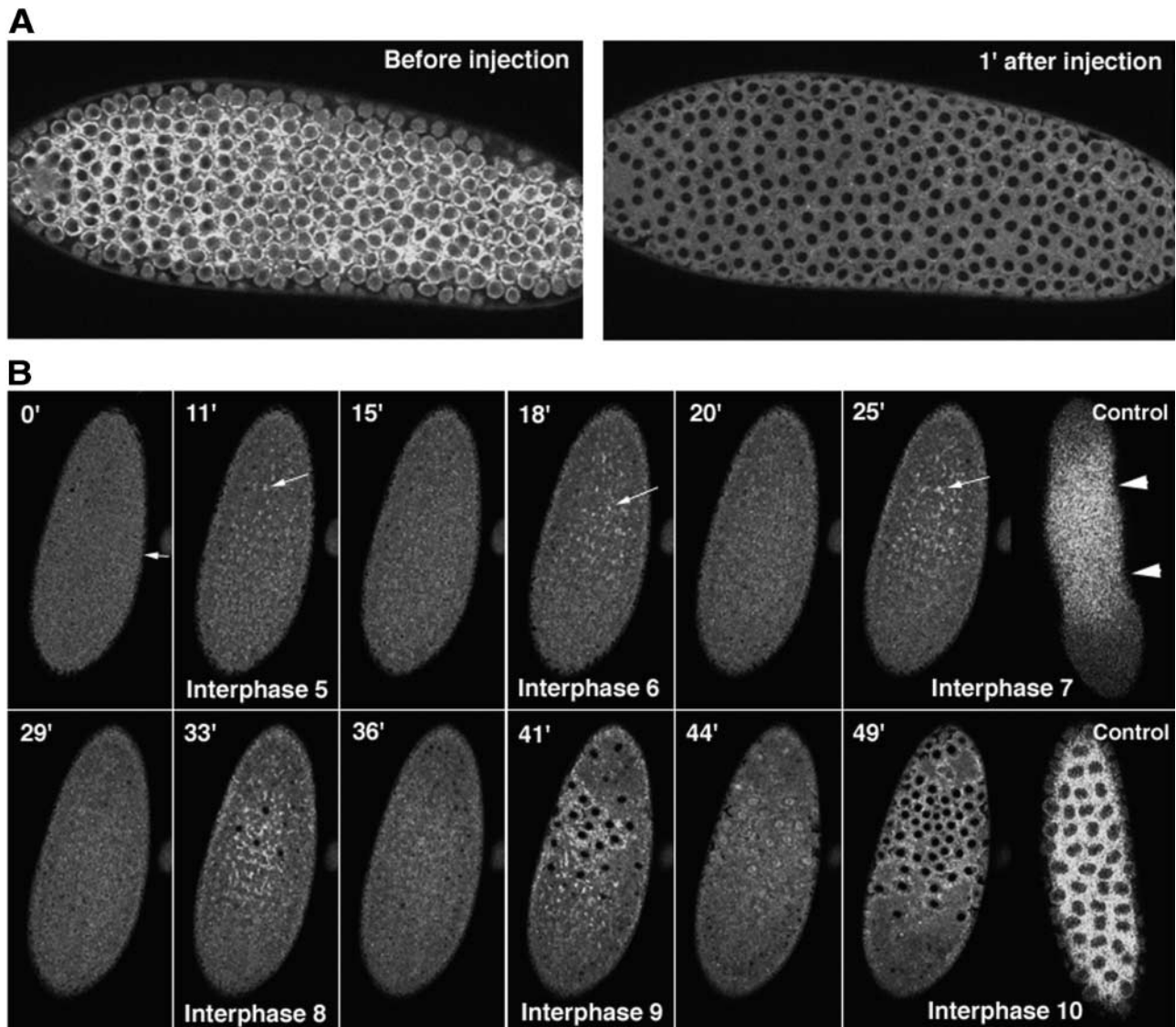
Figure 6. **Rho kinase inhibition affects cortical myosin recruitment, cortical contraction, and nuclear axial expansion.** (A) Injection of Y-27632 at interphase of cycle 12 induces a strong and rapid disappearance of cortical myosin. Surface of an RLC–GFP embryo was examined before (left) and 1 min after Y-27632 injection (right) during interphase of cycle 12. Before injection, RLC–GFP fluorescence strongly stained the cortex around the nuclei. 1 min after inhibition of Rho kinase by Y-2732, the cortical myosin fluorescence is dramatically reduced. (B) Injection of Y-27632 during early precortical divisions prevents cortical myosin cycling and induces a nuclear axial expansion defect. The surface of an RLC–GFP embryo was examined immediately after Y-27632 injection (first panel, arrow) at around cycle 3. During the mitotic cycles after injection, only faint, small, noncontiguous fluorescent patches appear and disappear at the cortex with each mitotic cycle (11', 18', and 25', arrow), and no cortical contractions occurs (compare with the control embryo in interphase 6). Nevertheless, these small myosin patches are found only in the cortical regions above the nuclear cloud. Moreover, the treated embryos display the two features of axial expansion failure: the nuclei reach the cortex precociously (approximately cycle 7), and they are unevenly distributed along the A/P axis, being clustered in the anterior half of the embryo. See video 8 available at http://www.jcb.org/cgi/content/full/jcb.200203148/DC1.

1997; Matsumura et al., 1998; Winter et al., 2001). Jordan and Karess (1997) showed that fly embryos expressing RLC lacking the activating phosphorylation sites were severely defective in axial expansion. To further test whether phosphorylation of these sites is required for myosin activity in nuclear axial expansion, we made use of a *sqh* transgene in which the primary (S21) and secondary (T20) activating sites were replaced with the phosphomimetic glutamic acid. Expressing one copy of this *sqhE20E21* transgene restored axial expansion in the leaky *sqh¹* germline clones, and moreover, substantially restored both oogenesis and subsequent axial expansion in null *sqh^{AX3}* germline clones (unpublished data). These genetic re-

sults show that phosphorylation of the RLC activating sites is required for myosin activity during nuclear axial expansion.

Rho kinase is a major determinant of the state of RLC phosphorylation, acting both to inhibit the myosin phosphatase and directly phosphorylate the activating serine and threonine (Amano et al., 1996; Kimura, et al., 1996; for review see Fukata et al. 2001). In *Drosophila*, a lethal mutation in the gene *drok* encoding rho kinase can be almost completely rescued by expression of the *sqhE20E21* transgene (Winter et al., 2001), indicating that RLC phosphorylation is the principle event regulated by *Drosophila* rho kinase (Drok) in vivo. To test whether Drok regulates myosin activity in the syncytial embryo, we used

the drug Y-27632, a specific Rho kinase inhibitor (for review see Narumiya et al. 2000). Within 1 min after injection of Y-27632 into an RLC–GFP blastoderm embryo during interphase, myosin largely disappeared from the cortex (Fig. 6 A). This result indicates that Drok activity is required to maintain myosin at the cortex during interphase.

When Y-27632 was injected into very young embryos, nearly all of the cyclic accumulation of cortical myosin was inhibited during the early syncytial divisions (Fig. 6 B; video 8 available at http://www.jcb.org/cgi/content/full/jcb.200203148/DC1). Only small dispersed patches of myosin still appeared during the interphases (Fig. 6 B, 11′, 18′, and 25′, arrows), and no cortical contractions occurred. Significantly, no axial nuclear expansion occurred (Fig. 6 B, 41′ and 49′). Without migrating evenly along the AP axis, the nuclei reached the cortex first at the anterocenter of the embryo. The small fragmented cortical myosin patches still recruited after Y-27632 injection were found only in the anterocentral region, precisely where the nuclei will reach the surface (Fig. 6 B). This observation provides further evidence that the extent and position of the nuclear cloud directly influence the recruitment of myosin to the adjacent cortex. In summary, inhibiting Rho kinase profoundly disrupts both axial nuclear migration and cyclic recruitment of myosin to the cortex and the subsequent cortical contraction, providing further evidence that these events are mechanistically linked.

Discussion

We have shown that during the early syncytial divisions of *Drosophila* embryogenesis, cytoplasmic myosin undergoes cycles of recruitment and dispersion in concert with the mitotic cycle. Each recruitment is associated with a cortical contraction, which is approximately coextensive with the cloud of syncytial nuclei, and is most likely required for the axial expansion of syncytial nuclei within the early embryo.

Changes in cortical myosin abundance with the mitotic cycle were first reported by Foe et al. (2000) based on their detailed studies of immunostained blastoderm stage embryos. They noted that cyclic changes in cortical myosin could be detected as early as cycle 8. Our results confirm and extend their observations by showing that (a) the cyclic recruitment of cortical myosin begins as early as interphase of cycle 4 and (b) recruitment is spatially and temporally regulated, being restricted to the cortical regions just above the expanding cloud of nuclei. When the spatial distribution of nuclei is perturbed (as following Y-27632 treatment), the cortical myosin is similarly affected. (c) Localized inhibition of Cdc2 activity locally promotes cortical myosin recruitment and (d) Cdc2 probably acts indirectly, and we provide evidence that Rho kinase may relay the Cdc2 signal to myosin.

Cdc2 activity indirectly regulates myosin dynamics

The present study clearly demonstrates that cycles of cortical myosin recruitment and dispersion are tightly regulated by Cdc2 activity. The temporally ectopic activation of Cdc2 (by GST–cyclin B injection) leads to a dispersion of myosin from the cortex, whereas premature inactivation of Cdc2 (by roscovitine inhibition) induces cortical myosin accumulation and contraction.

Satterwhite et al. (1992) reported that Cdc2 phosphorylates vertebrate myosin RLC in vitro on serines 1 and 2 and threonine 11, sites shown previously to inhibit myosin ATPase activity when phosphorylated by PKC (Bengur et al., 1987; Ikebe and Reardon, 1990). In vivo, Yamakita et al. (1994) demonstrated that S1 and S2 of RLC are highly phosphorylated in cells arrested at metaphase when Cdc2 activity is high. In contrast, the activating serine S19 is the predominant phosphorylated residue during cytokinesis after Cdc2 inactivation. These data suggested that Cdc2 could be directly involved in negatively regulating myosin activity during mitosis, inhibiting its premature activation at the future site of the cleavage furrow.

However, this model cannot explain the myosin dynamics we observe during the early divisions in *Drosophila* embryos, since mutant RLC (encoded by *sqh5XA*), lacking all possible serine and threonine targets of Cdc2, still functions normally and does not affect the cycles of cortical myosin recruitment and dispersion during early embryogenesis. Indeed, flies using *sqh5XA* as their only source of RLC are alive and fertile. Such results show that phosphorylation at these sites by Cdc2, or any other kinase, cannot be critical for myosin function and regulation. These results are in agreement with reports in fission yeast (McCollum et al., 1999) and echinoderm embryos (Shuster and Burgess, 1999), demonstrating that the inhibitory phosphorylation sites are not critical for myosin regulation in those systems. Together, these observations suggest that Cdc2 does not directly regulate myosin dynamics by phosphorylation of the RLC.

Rho kinase is a major regulator of RLC-activating phosphorylation (Amano et al., 1996; Fukata et al., 2001; Winter et al., 2001). We show that inhibition of Drok during blastoderm interphase induces a rapid and complete dispersion of myosin from the cortex, which suggests an activation of the myosin phosphatase (Fig. 6). Combined with the fact that expression of *sqhE20E21* is capable of rescuing a *drok*-null allele (Winter et al., 2001), these results strongly argue that Rho kinase regulates myosin cortical recruitment and contraction, both by inhibiting myosin phosphatase and by directly or indirectly promoting phosphorylation of the S21 activating site of RLC. Inhibition of Drok during precortical divisions also induces a defect in nuclear axial expansion, providing further evidence that myosin-based cortical contractions are responsible for nuclear axial expansion.

Cdc2 may indirectly regulate myosin dynamics via modulation of Drok activity. Drok itself contains no obvious consensus Cdc2 phosphorylation sites, so direct regulation by Cdc2 is unlikely. Cdc2 may regulate the local concentration of active Rho, for example, by regulating Rho GAP or Rho GEF activities. Cdc2 may also be regulating myosin in parallel to Drok. For instance, myosin phosphatase is reportedly stimulated by a mitosis-specific phosphorylation (Totsukawa et al., 1999).

Finally, Cdc2 may regulate actin recruitment to the cortex as well. Indeed, Foe et al. (2000) reported that actin also cycles to and from the cortex during syncytial cycle 8 and 9. In preliminary studies with a fluorescent probe for actin, we have observed in vivo cycles of localized cortical actin recruitment and dispersion beginning at mitotic cycle 4, just as is seen for myosin. Like myosin, the actin cycles are linked to nuclear position and mitotic phase, but they occur even in

sqh[1] germline clones (though in this case without the cortical contractions), indicating that they are independent of myosin activity (unpublished data). Independent recruitment of actin and myosin to the cortex provides two independent pathways for regulating myosin-based cortical contraction. This may explain in part how an otherwise constitutively active myosin incorporating RLC–E20E21 can function sufficiently well to rescue a *drok* mutant (Winter et al., 2001) or axial expansion.

A refined model for axial expansion

A functional link between nuclear axial expansion and myosin cortical recruitment and contraction is supported by the following observations: (a) the local cortical recruitment of myosin and contraction match very well both the position and extent of nuclear domain; (b) the contractions start at cycle 6 and occur during interphase and prophase, corresponding precisely to the timing of poleward nuclear migration (Baker et al., 1993); (c) treatments disrupting cortical contractions (*sqh* mutant germline clones or after vDrok inhibition by Y-26732) also provoke axial expansion failure.

Foe et al. (1993) presented a model for axial expansion in which the nuclei and their associated centrosomes expand spherically by microtubule-mediated mutual repulsion, but the stiffness of the cytogel formed by the cortical actin network forces the cloud of nuclei to expand laterally in an ellipsoid shape. Based on observations of F-actin dynamics and cytoplasmic movements in fixed and living embryos, von Dassow and Schubiger (1994) proposed that cytoplasmic streaming drives nuclear expansion along the A-P axis. They propose that the cytoplasmic movement is induced during interphase and prophase by a local disassembly of the actin network within the central cytoplasmic domain associated with the nuclei.

Both mechanisms may contribute to axial expansion, and neither is excluded by our data. We propose an extension of these models to include a dynamic cortical actin myosin network (Fig. 7). Coordinating myosin cortical assembly and contraction with the period of central domain actin filament disassembly (von Dassow and Schubiger, 1994) should maximize the cytoplasmic streaming to propel the nuclei polewards. Simultaneously, contraction of the cortical actin myosin network should stiffen the cytosol and thus further confine the centripetal movements of the nuclei, preventing their premature cortical migration. A satisfying feature of this model is that it readily explains why axial expansion does not begin until cycle 6 (something not obviously explicable by the first two models). Only at cycle 6 is sufficient myosin recruited to allow the first cortical contractions occur.

What regulates the spatial limits of the cortical myosin patch?

Why is myosin recruitment limited to the epi-nuclear cortical regions and why is myosin not recruited to the cortex before cycle 4? We believe this reflects the localized activation and inactivation of Cdc2 associated with the expanding nuclear region. Edgar et al. (1994) found that cyclin B levels and Cdc2 activity remain globally high during the first eight mitotic cycles. The authors proposed that during precortical divisions, local degradation of cyclin B associated with each dividing nucleus is sufficient to drive mitotic exit of individual
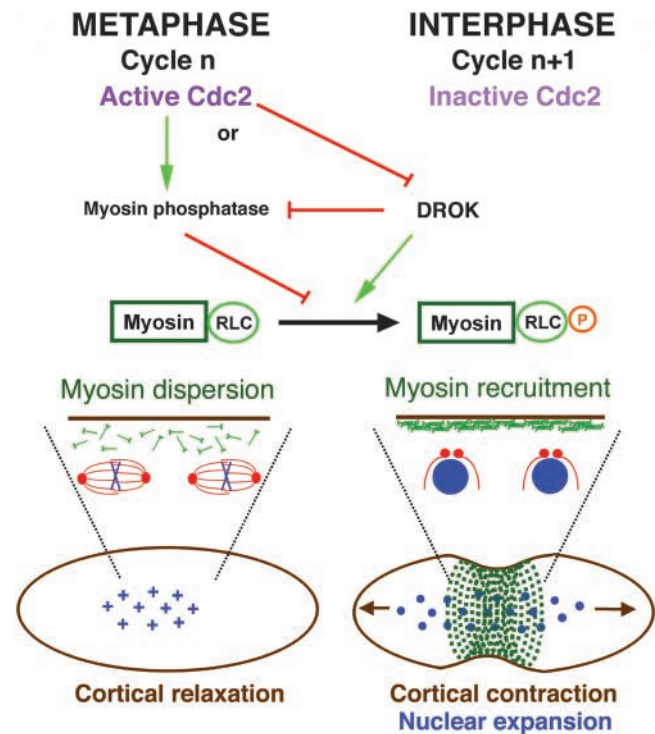

Figure 7.   **A model for cyclic cortical recruitment of myosin and its role in axial expansion.** In unfertilized eggs or during metaphase, Cdc2 activity is high. High Cdc2 levels inhibit the recruitment of myosin to the cortex by indirectly blocking the activating phosphorylation of RLC serine-21 by either inhibiting Rho kinase or activating myosin phosphatase. Interphase nuclei (right) have locally degraded their cyclin and therefore are associated with low Cdc2 levels. This in turn relieves the block on phosphorylation the RLC Ser-21, allowing the local assembly of active bipolar myosin in the cortex just above the nuclear cloud. The accumulation of active myosin provokes a cortical contraction, initiating a cytoplasmic current that carries the nuclei along the long axis toward the poles.

nuclei even though the cyclin B levels (and therefore Cdc2 activity) within the egg remain globally elevated. Su et al. (1998) demonstrated that during syncytial divisions, despite the constant global presence of cyclins and Cdc2 activity, proteolysis of cyclins is still essential for nuclei to exit mitosis. They proposed that there is a local change in Cdc2 activity through degradation of small local pools of cyclins associated with the mitotic apparatus. This has been confirmed recently by Huang and Raff (1999). The exclusion of cortical myosin from the region near the polar body (first noticed by Foe et al., [2000] and confirmed here) is particularly instructive. The polar body remains in metaphase, whereas the neighbor nuclei around it continue to cycle, demonstrating that mitotic physiology is at least partially autonomous even in the embryonic syncytium (Sullivan et al., 1993; Su et al., 1998). Because neither cortical recruitment nor dispersion of myosin requires microtubules (Figs. 3 and 4), we interpret the local absence of myosin near the polar body to its localized Cdc2 activity rather than to its robust microtubule array.

Thus, we propose that before cycle 4, as in unfertilized eggs, Cdc2 is active everywhere within the egg and inhibits myosin recruitment to the cortex. Starting at interphase cycle 4 or 5, the reduced cyclin concentration in the vicinity of the nuclear cloud (caused by cyclin degradation associated

with each mitotic apparatus) reduces local Cdc2 activity below the threshold required to inhibit phosphorylation of RLC on its activating sites. The activated myosin then forms bipolar filaments associated with the actin network in the cortex just above the cloud of nuclei, which in turn, starting at cycle 6, provokes the observed cortical contraction during interphase. This model is summarized in Fig. 7.

Conclusions

Myosin plays a major role in nuclear axial expansion during the first mitoses of the *Drosophila* embryo. Myosin undergoes a cycle of cortical recruitment and dispersion probably regulated by the phosphorylation state of its RLC, which in turn is tightly regulated by Cdc2 activity. These cycles induce a cortical contraction at interphase and relaxation at metaphase that may provoke a cytoplasmic flux to drive the nuclei toward the poles. In *Xenopus laevis* early embryos or artificially activated eggs, periodic surface contraction waves linked to cycles of cytoplasmic Cdc2 activation precede cleavage of the embryo (Rankin and Kirschner, 1997; Perez-Mongiovi et al., 1998). Although the molecular origin of these surface contraction waves is still unknown, the similarity to our observations in the *Drosophila* embryo strongly suggests that myosin dynamics are involved. Our data also share obvious similarities with the well-studied event of cytokinesis and suggest that phosphorylation of RLC activating sites at telophase might promote cortical myosin recruitment and be sufficient to initiate cortical contraction. Several reports provide evidence that phosphorylation of the RLC activating site causes cortical myosin recruitment to the equator and activate the contractile ring during cytokinesis (DeBiasio et al., 1996; Matsumura et al., 1998). Additionally, the inhibitory effect of Cdc2 on cytokinesis has been observed by Wheatley et al. (1997). However, the mechanism regulating myosin activity and recruitment to the contractile ring is still unclear. Our studies suggest that local inactivation of Cdc2 kinase near the cell membrane is sufficient to promote myosin recruitment to that specific region of the cortex and initiate a cortical contraction. Further study of this model system should shed light on the regulation of myosin dynamics during cytokinesis.

Materials and methods

Fly stocks
Flies ware raised on standard maize meal fly food at 25°C. *sqh¹* and *sqh^AX3* are described by Jordan and Karess (1997) and Karess et al. (1991). The stocks of *FRT101* and *ovoD1 FRT101/Y; hs-flp38* used to generate germline clones (Chou and Perrimon, 1992) were obtained from Dr. N. Perrimon (Harvard Medical School, Boston, MA). Wild-type controls used the stock *y w^67c*. The construction of the transgene *sqh-gfp* will be described elsewhere (unpublished data). The transgene *sqh-gfp* is expressed off the natural *sqh* promoter and rescues the *sqh^AX3*-null mutation in one copy, showing that the RLC–GFP fusion protein is fully functional. The stock *sqh^AX3*; P[w+ *sqh-gfp]42* in which the transgene is the only source of RLC was used for studying myosin behavior. The embryos produced by this strain are called "RLC–GFP embryos." The FLP–DFS system of Chou and Perrimon (1992) was used to generate homozygous *sqh¹* or *sqh^AX3* germline clones as described by Wheatley et al. (1995).

Mutant sqh5XA and sahE20E21 constructs
The mutant transgenes *sqh5XA* (*sqhA1A2A5A11A12)* and *sqhE20E21* were constructed by PCR using as template DNA the Bluescript SK+ vector (Stratagene) containing a 0.75-kb EcoR1 fragment of genomic *sqh⁺* (described by Jordan and Karess [1997] and Karess et al., [1991]). For *sqhE20E21,* a specific mutagenizing primer replacing T20 and S21 with glutamates was used.

For sqh5XA, three separate PCRs were done using three mutagenizing primers, replacing, respectively, S1S2, T5, and T11T12 with alanines. The second primer for each reaction was the universal sequencing primer. The resulting PCR products digested with appropriate restriction enzymes were used to replace the corresponding fragments in a wild-type 0.75-kb EcoRI fragment. The mutations were verified by sequencing. The mutated 0.75-kb fragment was assembled into an intact *sqh* gene controlled by its natural promoter in the P transformation vector CasPer (Pirrotta, 1988), which carries in addition the selectable marker *mini-white⁺*, and was introduced into the germ line of *y w^67* flies by standard methods (Ashburner, 1989).

Western blots
SDS-PAGE and immunoblotting were performed as described by Su (2000). Proteins were transferred to nitrocellulose membrane (Schleicher & Schuell). Protein blot was incubated with primary antibodies: rabbit anti-MHC antibody and mouse anti-GFP antibody (Medical and Biological Laboratories, Ltd.). Affinity-purified, HRP-conjugated goat antibodies against rabbit and mouse IgG (Santa Cruz Biotechnology, Inc.) and chemiluminescence reagent (ECL; Amersham Pharmacia Biotech) were used to detect primary antibodies.

Immunostaining
Fixation and immunostaining were performed as described by Foe et al. (2000). The postfix treatment was described by Rothwell and Sullivan (2000). The vitelline membranes were removed by hand with a needle under a binocular. Then, the embryos were incubated with the rabbit anti-MHC antibodies generated in our laboratory (Jordan and Karess, 1997) used at 1:1,000. Bound antibodies were detected using a goat anti–rabbit IgG secondary antibody conjugated to Alexa™ 488 (Molecular Probes). For propidium iodide staining, the embryos were treated with 10 μg/ml RNase for 2 h at 37°C followed by extensive rinsing in PBS and mounted in a 90% glycerol/PBS solution containing 1 μg/ml *N-N*-1–4-phenylenediamine and 1 mg/ml propidium iodide. For nuclear stages determination, 3 h collection embryos were fixed 40 min in heptane saturated with 37% formaldehyde and devitenillinazed by hand. The embryos were incubated with antihistone used at 1:500 (Chemicon). Bound antibody were detected using a goat anti–rabbit IgG secondary antibody conjugated to Alexa™ 488 (Molecular Probes). After rinsing in PBTA (PBS 1×, BSA 1%, Triton 0.05%, and azide 0.2%), the embryos were dehydrated with PBS/methanol (100:0, 20:80, 60:40, 40:60, 80:20, 0:100) and mounted in benzyl alcohol/benzyl benzoate (1:2) (Rothwell and Sullivan, 2000).

Microinjection and imaging of live embryos
RLC–GFP embryos were prepared for microinjection and TLCM according to Francis-Lang et al. (1999). The following reagents were injected at 50% egg length at approximately between 1 and 5% of the total egg volume: rhodamine-conjugated tubulin (Molecular Probes), colchicine (1 mM in H_2O) (Sigma-Aldrich), GST–cyclin B (6 mg/ml in 25 mM Hepes, 125 mM KCl, 10% glycerol) (a gift from Douglas Kellogg, University of California), roscovitine (10 mM in DMSO) (Meijer et al., 1997), Y-27632 (50 mM in H_2O) (Calbiochem), and DMSO (Sigma-Aldrich). Embryos were injected as described by Foe and Alberts (1983). Intracellular concentrations of the injected reagents were ~100-fold diluted. Scanning confocal movies were started within 20 s after injection.

Confocal microscopy and time-lapse recording
Microscopy was performed using a Leitz DMIRB inverted microscope equipped either with a Leica TCS NT or a Leica TCS SP2 laser confocal imaging system. Images of the time series result from three accumulations and were scanned every 15, 30, or 60 s.

Online supplemental material
The following videos are available at http://www.jcb.org/cgi/content/full/jcb.200203148/DC1. Video 1 shows myosin dynamics in vivo during precortical divisions (corresponds with Fig. 1). Videos 2 and 3 show cycles of myosin recruitment to the cortex correlating with mitotic cycles (correspond with Fig. 2, A and B, respectively). Video 4 demonstrates that myosin recruitment to the cortex is independent of microtubules (corresponds with Fig. 3 A). Myosin dynamics are recorded after colchicine injection at anaphase of cycle 12. Video 5 demonstrates that cortical myosin recruitment to the cortex depends on cyclin B degradation (corresponds with Fig. 3 B). Myosin dynamics after injection of a stable form of cyclin B at anaphase of cycle 12 are shown. Video 6 demonstrates that Cdc2 inactivation by roscovitine leads to cortical myosin recruitments (corresponds with Fig. 4 A). Video 7 shows that cortical myosin distribution is dependent on Cdc2 activity (corresponds with Fig. 4 B). Video 8 shows how Rho kinase

inhibition affects cortical myosin cycles, cortical contraction, and nuclear axial expansion (corresponds with Fig. 6 B).

References

Amano, M., M. Ito, K. Kimura, Y. Fukata, K. Chihara, T. Nakano, Y. Matsuura, and K. Kaibuchi. 1996. Phosphorylation and activation of myosin by Rho-associated kinase (Rho-kinase). *J. Biol. Chem.* 271:20246–20249.

Ashburner, M. 1989. *Drosophila*: A Laboratory Handbook. Cold Spring Harbor Laboratory Press, Cold Spring Harbor, NY.

Baker, J., W.E. Theurkauf, and G. Schubiger. 1993. Dynamic changes in microtubule configuration correlate with nuclear migration in the preblastoderm *Drosophila* embryo. *J. Cell Biol.* 122:113–121.

Bengur, A.R., E.A. Robinson, E. Appella, and J.R. Sellers. 1987. Sequence of the sites phosphorylated by protein kinase C in the smooth muscle myosin light chain. *J. Biol. Chem.* 262:7613–7617.

Bresnick, A.R. 1999. Molecular mechanisms of nonmuscle myosin-II regulation. *Curr. Opin. Cell Biol.* 11:26–33.

Chou, T.B., and N. Perrimon. 1992. Use of a yeast site-specific recombinase to produce female germline chimeras in *Drosophila*. *Genetics.* 131:643–653.

DeBiasio, R.L., G.M. LaRocca, P.L. Post, and D.L. Taylor. 1996. Myosin II transport, organization, and phosphorylation: evidence for cortical flow/solation-contraction coupling during cytokinesis and cell locomotion. *Mol. Biol. Cell.* 7:1259–1282.

Edgar, B.A., F. Sprenger, R.J. Duronio, P. Leopold, and P.H. O'Farrell. 1994. Distinct molecular mechanism regulate cell cycle timing at successive stages of *Drosophila* embryogenesis. *Genes Dev.* 8:440–452.

Foe, V.E., and B.M. Alberts. 1983. Studies of nuclear and cytoplasmic behaviour during the five mitotic cycles that precede gastrulation in *Drosophila* embryogenesis. *J. Cell Sci.* 61:31–70.

Foe, V.E., G.M. Odell, and B.A. Edgar. 1993. Mitosis and morphogenesis in the *Drosophila* embryo: point and counterpoint. *In* The Development of *Drosophila*. Vol. 1. M. Bate and A. Martinez Arias, editors. Cold Spring Harbor Laboratory Press, Cold Spring Harbor, NY. 149–300.

Foe, V.E., C.M. Field, and G.M. Odell. 2000. Microtubules and mitotic cycle phase modulate spatiotemporal distributions of F-actin and myosin II in *Drosophila* syncytial blastoderm embryos. *Development.* 127:1767–1787.

Francis-Lang, H., J. Minden, W. Sullivan, and K. Oegema. 1999. Live confocal analysis with fluorescently labeled proteins. *Methods Mol. Biol.* 122:223–239.

Fukata, Y., M. Amano, and K. Kaibuchi. 2001. Rho-Rho-kinase pathway in smooth muscle contraction and cytoskeletal reorganization of non-muscle cells. *Trends Pharmacol. Sci.* 22:32–39.

Hatanaka, K., and M. Okada. 1991. Retarded nuclear migration in *Drosophila* embryos with aberrant F-actin reorganization caused by maternal mutations and by cytochalasin treatment. *Development.* 111:909–920.

Huang, J, and J.W. Raff. 1999. The disappearance of cyclin B at the end of mitosis is regulated spatially in *Drosophila* cells. *EMBO J.* 18:2184–2195.

Ikebe, M., and S. Reardon. 1990. Phosphorylation of bovine platelet myosin by protein kinase C. *Biochemistry.* 29:2713–2720.

Jordan, P., and R. Karess. 1997. Myosin light chain-activating phosphorylation sites are required for oogenesis in *Drosophila*. *J. Cell Biol.* 139:1805–1819.

Karess, R.E., X.J. Chang, K.A. Edwards, S. Kulkarni, I. Aguilera, and D.P. Kiehart. 1991. The regulatory light chain of nonmuscle myosin is encoded by spaghetti-squash, a gene required for cytokinesis in *Drosophila*. *Cell.* 65:1177–1189.

Kimura, K., M. Ito, M. Amano, K. Chihara, Y. Fukata, M. Nakafuku, B. Yamamori, J. Feng, T. Nakano, K. Okawa, et al. 1996. Regulation of myosin phosphatase by Rho and Rho-associated kinase (Rho-kinase). *Science.* 273:245–248.

Matsumura, F., S. Ono, Y. Yamakita, G. Totsukawa, and S. Yamashiro. 1998. Specific localization of serine 19 phosphorylated myosin II during cell locomotion and mitosis of cultured cells. *J. Cell Biol.* 140:119–129.

McCollum, D., A. Feoktistova, and K.L. Gould. 1999. Phosphorylation of the myosin-II light chain does not regulate the timing of cytokinesis in fission yeast. *J. Biol. Chem.* 274:17691–17695.

Meijer, L., A. Borgne, O. Mulner, J.P. Chong, J.J. Blow, N. Inagaki, M. Inagaki, J.G. Delcros, and J.P. Moulinoux. 1997. Biochemical and cellular effects of roscovitine, a potent and selective inhibitor of the cyclin-dependent kinases cdc2, cdk2 and cdk5. *Eur. J. Biochem.* 243:527–536.

Narumiya, S., T. Ishizaki, and M. Uehata. 2000. Use and properties of ROCK-specific inhibitor Y-27632. *Methods Enzymol.* 325:273–284.

Perez-Mongiovi, D., P. Chang, and E. Houliston. 1998. A propagated wave of MPF activation accompanies surface contraction waves at first mitosis in *Xenopus*. *J. Cell Sci.* 111:385–393.

Pirrotta, V. 1988. Vectors for P-mediated transformation in *Drosophila*. *Biotechnology.* 10:437–456.

Rankin, S., and M.W. Kirschner. 1997. The surface contraction waves of *Xenopus* eggs reflect the metachronous cell-cycle state of the cytoplasm. *Curr. Biol.* 7:451–454.

Rothwell, W.F., and W. Sullivan. 2000. Fluorescent analysis of *Drosophila* embryos. *In Drosophila* Protocils. W. Sullivan, M. Ashburner, and R.S. Hawley, editors. Cold Spring Harbor Laboratory Press, Cold Spring Harbor, NY. 141–157.

Satterwhite, L.L., M.J. Lohka, K.L. Wilson, T.Y. Scherson, L.J. Cisek, J.L. Corden, and T.D. Pollard. 1992. Phosphorylation of myosin-II regulatory light chain by cyclin-p34cdc2: a mechanism for the timing of cytokinesis. *J. Cell Biol.* 118:595–605.

Sellers, J.R. 1991. Regulation of cytoplasmic and smooth muscle myosin. *Curr. Opin. Cell Biol.* 3:98–104.

Shuster, C.B., and D.R. Burgess. 1999. Parameters that specify the timing of cytokinesis. *J. Cell Biol.* 146:981–992.

Su, T.T. 2000. Immunoblotting of proteins from single *Drosophila* embryos. *In Drosophila* Protocols. W. Sullivan, M. Ashburner, and R.S. Hawley, editors. Cold Spring Harbor Laboratory Press, Cold Spirng Harbor, NY. 577–583.

Su, T.T., F. Sprenger, P.J. DiGregorio, S.D. Campbell, and P.H. O'Farrell. 1998. Exit from mitosis in *Drosophila* syncytial embryos requires proteolysis and cyclin degradation, and is associated with localized dephosphorylation. *Genes Dev.* 12:1495–1503.

Sullivan, W., D.R. Daily, P. Fogarty, K.J. Yook, and S. Pimpinelli. 1993. Delays in anaphase initiation occur in individual nuclei of the syncytial *Drosophila* embryo. *Mol. Biol. Cell.* 4:885–896.

Tan, J.L., S. Ravid, and J.A. Spudich. 1992. Control of nonmuscle myosins by phosphorylation. *Annu. Rev. Biochem.* 61:721–759.

Taubman, M.B., J.W. Grant, and B. Nadal-Ginard. 1987. Cloning and characterization of mammalian myosin regulatory light chain (RLC) cDNA: the RLC gene is expressed in smooth, sarcomeric, and nonmuscle tissues. *J. Cell Biol.* 104:1505–1513.

Totsukawa, G., Y. Yamakita, S. Yamashiro, H. Hosoya, D.J. Hartshorne, and F. Matsumura. 1999. Activation of myosin phosphatase targeting subunit by mitosis-specific phosphorylation. *J. Cell Biol.* 144:735–744.

von Dassow, G., and G. Schubiger. 1994. How an actin network might cause fountain streaming and nuclear migration in the syncytial *Drosophila* embryo. *J. Cell Biol.* 127:1637–1653.

Wheatley, S., S. Kulkarni, and R. Karess. 1995. *Drosophila* nonmuscle myosin II is required for rapid cytoplasmic transport during oogenesis and for axial nuclear migration in early embryos. *Development.* 121:1937–1946.

Wheatley, S.P., E.H. Hinchcliffe, M. Glotzer, A.A. Hyman, G. Sluder, and Y. Wang. 1997. CDK1 inactivation regulates anaphase spindle dynamics and cytokinesis in vivo. *J. Cell Biol.* 138:385–393.

Winter, C.G., B. Wang, A. Ballew, A. Royou, R. Karess, J.D. Axelrod, and L. Luo. 2001. *Drosophila* Rho-associated kinase (Drok) links Frizzled-mediated planar cell polarity signaling to the actin cytoskeleton. *Cell.* 105:81–91.

Yamakita, Y., S. Yamashiro, and F. Matsumura. 1994. In vivo phosphorylation of regulatory light chain of myosin II during mitosis of cultured cells. *J. Cell Biol.* 124:129–137.

Zalokar, M., and I. Erk. 1976. Division and migration of nuclei during early embryogenesis of *Drosophila* melanogaster. *J. Microsc. Biol. Cell.* 25:97–106.